



Management of Drug Interactions with Inducers: Onset and Disappearance of Induction on Cytochrome P450 3A4 and Uridine Diphosphate Glucuronosyltransferase 1A1 Substrates

Sara Bettonte^{1,2} · Mattia Berton^{1,2} · Felix Stader³ · Manuel Battegay^{1,2} · Catia Marzolini^{1,2,4}

Accepted: 14 May 2023 / Published online: 6 June 2023
© The Author(s) 2023

Abstract

Background People living with HIV may present co-morbidities requiring the initiation and subsequently the discontinuation of medications with inducing properties. The time to reach maximal enzyme induction and to return to baseline enzyme levels has not been thoroughly characterized.

Objective The aim of this study was to evaluate the onset and disappearance of dolutegravir [uridine diphosphate glucuronosyltransferase (UGT) 1A1 and cytochrome P450 (CYP) 3A4 substrate] and raltegravir (UGT1A1 substrate) induction with strong and moderate inducers using physiologically based pharmacokinetic (PBPK) modeling.

Methods The predictive performance of the PBPK model to simulate dolutegravir and raltegravir pharmacokinetics and to reproduce the strength of induction was verified using clinical drug–drug interaction studies (steady-state induction) and switch studies (residual induction). The model was considered verified when the predictions were within 2-fold of the observed data. One hundred virtual individuals (50% female) were generated to simulate the unstudied scenarios. The results were used to calculate the fold-change in CYP3A4 and UGT1A1 enzyme levels upon initiation and discontinuation of strong (rifampicin) or moderate (efavirenz or rifabutin) inducers.

Results The time for reaching maximal induction and subsequent disappearance of CYP3A4 induction was 14 days for rifampicin and efavirenz but 7 days for rifabutin. The distinct timelines for the moderate inducers relate to their different half-lives and plasma concentrations. The induction and de-induction processes were more rapid for UGT1A1.

Conclusions Our simulations support the common practice of maintaining the adjusted dosage of a drug for another 2 weeks after stopping an inducer. Furthermore, our simulations suggest that an inducer should be administered for at least 14 days before conducting interaction studies to reach maximal induction.

Key Points

Our simulations indicate that at least 14 days are needed to reach maximal induction and to return to CYP3A4 baseline enzymes levels in the presence of an inducer. This implies that an inducer should be administered for at least 14 days before conducting drug–drug interaction studies to reach maximal induction.

Our results also support the common practice of maintaining the adjusted dosage of a drug for another 2 weeks upon discontinuation of an inducer.

The time to reach maximal induction and resolution of induction is shorter for UGT1A1.

✉ Sara Bettonte
sara.bettonte@unibas.ch

✉ Catia Marzolini
catia.marzolini@usb.ch

¹ Division of Infectious Diseases and Hospital Epidemiology, Departments of Medicine and Clinical Research, University Hospital Basel, Petersgraben 4, 4031 Basel, Switzerland

² Faculty of Medicine, University of Basel, 4031 Basel, Switzerland

³ Certara UK Limited, Sheffield, UK

⁴ Department of Molecular and Clinical Pharmacology, University of Liverpool, Liverpool L69 3GF, UK

1 Introduction

Potent antiretroviral drugs (ARVs) dramatically changed the prognosis of HIV-infection. Treated people living with HIV (PLWH) have a life expectancy that is close, if not identical, to people without HIV infection [1]. Thus, the management of drug–drug interactions (DDIs) with ARVs represents a key clinical activity considering that most PLWH may develop at least one comorbidity during their lifespan. ARVs have considerably improved over the years and have a notably lower propensity to cause DDIs; however, several first-line ARVs are subject to DDIs with inducers of drug metabolizing enzymes [i.e., cytochrome P450 (CYP) and uridine diphosphate glucuronosyltransferase (UGT)] [2].

The induction of drug metabolizing enzymes occurs upon the binding of a drug to a nuclear receptor [i.e., pregnane X receptor (PXR), constitutive androstane receptor (CAR) or aryl hydrocarbon receptor (AhR)]. PXR is involved in the upregulation of CYP3A4 and UGTs expression. Following the heterodimerization with the 9-*cis*-retinoic acid receptor (RXR), the RXR-PXR complex interacts with response elements of target genes leading to the transcription of mRNA encoding the drug metabolizing enzymes [3, 4]. Thus, induction takes several days to fully develop and to disappear upon initiation and discontinuation of an inducer. This statement is supported by a clinical DDI study showing notably that the moderate inducer efavirenz reduced rilpivirine (CYP3A4 substrate) area under the concentration–time curve (AUC_t) by 46% and 18% at days 1 and 14, respectively, post-discontinuation of efavirenz [5]. However, it is unclear whether the time to reach maximal induction and resolution of induction varies depending on the inducer strength and elimination half-life ($t_{1/2}$) or on the degradation rate of the metabolic enzyme. This question is of particular interest as the first-line ARVs dolutegravir (metabolism by UGT1A1 > CYP3A4) or raltegravir (UGT1A1) require a dose adjustment when co-administered with strong inducers as does doravirine (CYP3A4) when given with moderate inducers [6–8]. It is common practice to maintain the adjusted dosage of the ARV for another 2 weeks after the last dose of the inducer, regardless of the properties of the inducer or the enzyme involved in the metabolism of the ARV. However, data to support this practice are missing.

Physiologically based pharmacokinetic (PBPK) modeling has demonstrated its predictive power to simulate clinically relevant yet unstudied DDI scenarios [9, 10]. PBPK modeling combines *in vitro* data and clinically observed data to simulate pharmacokinetics in virtual individuals. The virtual population used to inform the PBPK model is developed based on observed blood flows, organ weights, and other physiological parameters required to simulate drug disposition. To date, PBPK modeling has been applied to investigate

the time needed for CYP3A4 enzyme levels to return to baseline after stopping the strong inducer rifampicin; however, no data are available for moderate inducers or for the recovery of UGT1A1 abundance [11, 12].

Since dolutegravir is metabolized by UGT1A1 and CYP3A4 [13] and raltegravir by UGT1A1 [14], we selected these ARVs to investigate the time required for CYP3A4 and UGT1A1 abundances to return to baseline after stopping rifampicin ($t_{1/2}$ 2–3 h [15]) or after discontinuing two moderate inducers with distinct half-lives, namely efavirenz ($t_{1/2}$ 40–55 h after multiple doses [16]) and rifabutin ($t_{1/2}$ 45 h [17]). We also investigated the time to reach maximal induction of CYP3A4 and UGT1A1 upon initiation of rifampicin, efavirenz and rifabutin.

2 Methods

We took a 3-step approach. First, we evaluated the performance of the PBPK model to simulate the pharmacokinetics of each individual drug against observed clinical data after intravenous and oral administration. Second, we verified that the model correctly reproduces the strength of induction using available DDI studies (reflecting steady-state induction) and switch studies (reflecting residual induction). Third, we used the fully verified PBPK model to simulate the unstudied scenarios. Each scenario included 100 virtual individuals (50% female) between 20 and 50 years of age. For all the scenarios simulated, we considered the changes in enzyme levels rather than the activity (clearance); however, it should be noted that these parameters are correlated (i.e., an increase in enzyme levels correlates with an increase in clearance).

2.1 PBPK Model and Drug Model Development

Our in-house PBPK model was built in Matlab[®]2020a (MathWorks, Natick, MA, USA) [18]. In order to generate a cohort of virtual individuals, the model was informed with equations previously developed by our group describing the physiological changes in a Caucasian healthy population aged 20–99 years [19]. The equations are presented in Supplementary Table 2. The drug models were developed using published *in vitro* physicochemical parameters of each drug or, if the data were not available, using *in silico* predictions. The model parameters for dolutegravir, raltegravir, rifampicin, efavirenz, and rifabutin are summarized in Supplementary Table 1. The model performance to predict the pharmacokinetics was evaluated for intravenous and oral administration, and the model was considered verified when the predictions were within 2-fold of the observed clinical data (Data on file; Bettonte et al.) [20, 21].

2.2 Model Verification Against Observed DDI and Switch Studies

The fraction of dolutegravir metabolism by UGT1A1 and CYP3A4 and the fraction of raltegravir metabolized by UGT1A1, as well as the strength of induction were verified against published DDI clinical studies in which the pharmacokinetics of dolutegravir or raltegravir were measured in the absence and in the presence of rifampicin, efavirenz, or rifabutin after steady-state administration [22–26]. In addition, published switch studies were used to verify the performance of the PBPK model to predict the residual induction after stopping efavirenz; therefore, the pharmacokinetics of the CYP3A4 substrate rilpivirine dosed at 25 mg and the UGT1A1/CYP3A4 substrate dolutegravir dosed at 50 mg were simulated on different days following efavirenz discontinuation [5, 27]. The model was considered to be verified when the simulations were within 2-fold, as described in the PBPK guidelines [28, 29]. We also used the more stringent criterion proposed by Guest et al. for the verification of all the DDI scenarios [30]. Finally, the change in CYP3A4 and UGT1A1 enzyme levels during and after stopping the administration of efavirenz were visually checked to extrapolate the time needed to return to baseline enzyme levels. The 1.25-fold induction threshold was considered as the limit below which the ratio of the AUC (i.e., AUC in the presence vs. the absence of a perpetrator), was outside the no-boundary efficacy limit of 0.8.

2.3 Model Simulations of Unknown Clinical Scenarios

A cohort of 100 virtual individuals aged 20–50 (50% female) was generated to simulate the unknown scenarios presented in Table 1 and Table 2. The study design of de Wet et al. [27], in which dolutegravir (50 mg once daily) was initiated 12 h after stopping efavirenz, was applied first to verify the residual induction on dolutegravir on days 7, 14, and 28 post-efavirenz dosing. This same dosing schedule was subsequently used to simulate dolutegravir pharmacokinetics following the discontinuation of rifampicin or rifabutin, and the pharmacokinetics of raltegravir during the switch scenario from rifampicin, efavirenz, or rifabutin. The DDI ratio (reflecting the residual induction) was calculated as the ratio of the trough concentration (C_{trough}) and AUC_{τ} in the presence versus the absence of the residual inducing effect of rifampicin, efavirenz, or rifabutin. As described in Sect. “Model Verification Against Observed DDI and Switch Studies”, the changes in CYP3A4 and UGT1A1 enzyme levels were visually checked and the time to return to baseline (i.e., below the 1.25-fold induction threshold) was extrapolated.

2.4 Sensitivity Analysis

The disappearance of the inducing effect is governed by the $t_{1/2}$ of the perpetrator and by the degradation constant (K_{deg}) of the enzyme, which correlates with $t_{1/2}$ of the enzyme [31]. Since this parameter has not been measured in humans, the K_{deg} value for UGT1A1 implemented in our in-house PBPK model was derived from a rat model [32]. Therefore, we conducted a sensitivity analysis to determine how changes in the K_{deg} UGT1A1 value impact the residual induction effect of rifampicin on raltegravir (UGT1A1 substrate) AUC, and C_{trough} at days 1, 7, 14, and 28 post-rifampicin dosing. For this analysis, we considered the situation of a single male individual aged 35 years old [body mass index (BMI) 25 kg/m²] and we modified by 1% the original UGT1A1 K_{deg} value reported in the literature [32]. The impact of K_{deg} on the PBPK model uncertainty was calculated using Eq. 1 [33]:

$$\text{Sensitivity coefficient} = \frac{\frac{d_1 - d_0}{d_0}}{\frac{p_1 - p_0}{p_0}} \quad (1)$$

where d_0 is the model-predicted dose metric of interest (i.e., AUC and C_{trough}) with the original parameter value, d_1 is the model-predicted dose metric of interest (i.e., AUC and C_{trough}) with a 1% increase in parameter value, p_0 is the original parameter value (i.e., K_{deg}), and p_1 is the parameter value with a 1% increase (i.e., K_{deg}).

The model uncertainty was evaluated using the criteria defined by Teeguarden et al. [33, 34]:

- Low: sensitivity coefficient is between 0.1 and 0.15. Low model uncertainty is obtained when the available data are measured in the correct species, the coefficient of variation (CV) is less than 0.5, or the parameter was successfully verified using PBPK modeling.
- Medium: sensitivity coefficient is between 0.15 and 0.5. Medium model uncertainty can present with data scaled from a different species, but for which the scaling holds across species.
- High: sensitivity coefficient is greater than 0.5. High model uncertainty can present when the parameter of interest is not available.

3 Results

3.1 Drug Model Development

The PBPK model was able to predict the pharmacokinetics of all evaluated drugs within 2-fold of the observed clinical data. The simulations of the various drugs as well as the

Table 1 Effect of residual induction on dolutegravir pharmacokinetics at days 1, 7, 14, and 28 post-rifampicin, efavirenz, and rifabutin dosing

	Absence inducer			After stopping inducer			DDI ratio (residual induction)			Reference
	Observed	Predicted	Ratio P/O	Observed	Predicted	Ratio P/O	Observed	Predicted	Ratio P/O	
	Dolutegravir—day 1 after stopping rifampicin									
C_{trough} [ng/mL]	–	749 (50)	–	–	62 (109)	–	–	0.08	–	–
AUC_{0-24} [ng×h/mL]	–	35,677 (26)	–	–	15,549 (38)	–	–	0.44	–	–
Dolutegravir—day 7 after stopping rifampicin										
C_{trough} [ng/mL]	–	1068 (69)	–	–	431 (79)	–	–	0.40	–	–
AUC_{0-24} [ng×h/mL]	–	52,295 (45)	–	–	32,154 (42)	–	–	0.61	–	–
Dolutegravir—day 14 after stopping rifampicin										
C_{trough} [ng/mL]	–	1070 (70)	–	–	806 (70)	–	–	0.75	–	–
AUC_{0-24} [ng×h/mL]	–	52,391 (46)	–	–	44,172 (43)	–	–	0.84	–	–
Dolutegravir—day 28 after stopping rifampicin										
C_{trough} [ng/mL]	–	1070 (70)	–	–	1046 (69)	–	–	0.98	–	–
AUC_{0-24} [ng×h/mL]	–	52,391 (46)	–	–	51,624 (46)	–	–	0.99	–	–
Dolutegravir—day 1 after stopping efavirenz										
C_{trough} [ng/mL]	–	910 ± 456	–	–	435 ± 332	–	–	0.48	–	–
AUC_{0-24} [ng×h/mL]	–	37,681 ± 9941	–	–	27,141 ± 8807	–	–	0.72	–	–
Dolutegravir—day 7 after stopping efavirenz										
C_{trough} [ng/mL]	–	1497 ± 1050	–	938 ± 955	948 ± 698	–	1.01	0.63	–	[27]
AUC_{0-24} [ng×h/mL]	–	60,683 ± 28,494	–	–	45,429 ± 19,778	–	–	0.75	–	–
Dolutegravir—day 14 after stopping efavirenz										
C_{trough} [ng/mL]	–	1505 ± 1070	–	861 ± 627	1217 ± 833	–	1.41	0.81	–	[27]
AUC_{0-24} [ng×h/mL]	–	60,961 ± 29,091	–	–	53,111 ± 23,105	–	–	0.87	–	–
Dolutegravir—day 28 after stopping efavirenz										
C_{trough} [ng/mL]	–	1505 ± 1071	–	1219 ± 710	1428 ± 977	–	1.17	0.95	–	[27]
AUC_{0-24} [ng×h/mL]	–	60,966 ± 29,113	–	–	58,909 ± 26,763	–	–	0.97	–	–
Dolutegravir—day 1 after stopping rifabutin										
C_{trough} [ng/mL]	–	749 (50)	–	–	554 (54)	–	–	0.74	–	–
AUC_{0-24} [ng×h/mL]	–	35,677 (26)	–	–	31,539 (27)	–	–	0.88	–	–
Dolutegravir—day 7 after stopping rifabutin										
C_{trough} [ng/mL]	–	1068 (69)	–	–	934 (67)	–	–	0.87	–	–
AUC_{0-24} [ng×h/mL]	–	52,294 (45)	–	–	48,073 (43)	–	–	0.92	–	–
Dolutegravir—day 14 after stopping rifabutin										
C_{trough} [ng/mL]	–	1070 (70)	–	–	1029 (69)	–	–	0.96	–	–
AUC_{0-24} [ng×h/mL]	–	52,390 (46)	–	–	51,090 (45)	–	–	0.98	–	–
Dolutegravir—day 28 after stopping rifabutin										
C_{trough} [ng/mL]	–	1070 (70)	–	–	1067 (70)	–	–	1.00	–	–
AUC_{0-24} [ng×h/mL]	–	52,391 (46)	–	–	52,288 (46)	–	–	1.00	–	–

The results are represented as geometric mean (CV), unless otherwise specified as mean ± SD

AUC_{0-24} area under the concentration–time curve to tau; C_{trough} trough concentration; *DDI* drug–drug interaction; *O* observed; *P* predicted

observed clinical data have been previously published by our group (Data on file; Bettonte et al.) [20, 21].

3.2 Model Verification Against Observed DDI and Switch Studies

The model correctly predicted the fraction of UGT1A1 and CYP3A4 metabolism for dolutegravir, as the DDI between dolutegravir and rifampicin, efavirenz, or rifabutin were simulated within 2-fold of the observed data, as shown in Supplementary Table 3. Furthermore, the predicted versus observed ratio for AUC, and C_{trough} were within the upper and lower limits defined by Guest et al. [30]. However, the ratio for the peak concentration (C_{max}) was outside the upper and lower limits because the clinical study paradoxically reported an increase in dolutegravir C_{max} [22], even though rifabutin is an inducer (Supplementary Fig. 1). Similarly, for raltegravir, the observed C_{max} and AUC used for the criterion proposed by Guest et al. [30] reflected an inhibition effect rather than induction [26] (Supplementary Fig. 1); however, the ratio for C_{trough} was within the upper and lower limits proposed by Guest et al. [30] (Supplementary Fig. 1). Finally, as for dolutegravir, all the DDI predictions between raltegravir and rifampicin, efavirenz, or rifabutin were within 2-fold of the clinical observed data (Supplementary Table 3). The PBPK model predicted, also correctly, the residual inducing effect on dolutegravir pharmacokinetics at days 7, 14, and 28 (Table 1) post-efavirenz dosing. The performance of the PBPK model to reproduce residual induction was also verified using clinical data from the efavirenz to rilpivirine switch study [5]. The simulated rilpivirine pharmacokinetic parameters were within 2-fold of the observed clinical data at days 1, 14, 21 post-efavirenz dosing (Supplementary Table 4) and borderline for the upper and lower limits proposed by Guest et al. (Data on file; Bettonte et al) [30] (Supplementary Fig. 2). The simulation results showed that, upon initiation of efavirenz, the mean maximal induction of CYP3A4 was reached after 19 days (Fig. 1b) and the one of UGT1A1 after 7 days (Fig. 1e). Upon discontinuation of efavirenz, 14 days were necessary for the CYP3A4 enzyme level to go below the 1.25-fold threshold (Fig. 1b). However, when considering the population variability, 69% of the individuals were predicted to have reached the 1.25-fold CYP3A4 abundance threshold at this time point. On the other hand, the UGT1A1 enzyme level was predicted to require 7 days to return close to the baseline enzyme level, with 72% of individuals predicted to achieve the 1.25-fold abundance threshold by this time point (Fig. 1e).

3.3 Model Simulations of Unknown Clinical Scenarios

The residual inducing effect of rifampicin was predicted to decrease dolutegravir AUC_{τ} by 56% and 39% at days 1 and 7 post-dosing, respectively. The mitigation of the rifampicin-inducing effect was apparent after 14 days as the decrease in dolutegravir AUC_{τ} was predicted to be minimal (16%), and negligible (1%) after 28 days (Table 1). On the other hand, the residual-inducing effect of rifampicin was more pronounced on dolutegravir C_{trough} , as it was predicted to be decreased by 92% and 60% on days 1 and 7, respectively. A 25% reduction in dolutegravir C_{trough} was still predicted at day 14 post-dosing, but it was negligible at day 28 (Table 1). The simulation results showed that the residual induction of rifampicin reduced raltegravir AUC_{τ} and C_{trough} by 15% and 22%, respectively, on day 1 post-dosing; however, the inducing effect was negligible after 7 days (Table 2). As depicted in Fig. 1a, rifampicin was predicted to require at least 14 days of continuous administration to reach near-maximal induction of CYP3A4. After stopping rifampicin, 18 days were necessary for 55% of the individuals to reach the 1.25-fold abundance threshold. Regarding UGT1A1, the steady-state and the time to go back to the baseline abundance were predicted to be faster than with CYP3A4 (Fig. 1d).

The residual inducing effect of rifabutin was predicted to decrease dolutegravir AUC_{τ} and C_{trough} by 12% and 26%, respectively, on day 1 post-dosing. The AUC_{τ} was still reduced by 8% and C_{trough} by 13% 7 days after stopping rifabutin. However, the induction was negligible after 14 days (reduction in AUC_{τ} and C_{trough} by 2% and 4%, respectively) (Table 1). The simulation results showed that upon discontinuation of rifabutin, the raltegravir AUC_{τ} and C_{trough} were reduced by 3% and 5%, respectively, 1 day post-dosing. The residual induction effect of rifabutin is negligible 7 days post-discontinuation (Table 2). Upon initiation of rifabutin, near-maximal CYP3A4 induction was predicted to be reached in 10 days (Fig. 1c) and in 1 day for UGT1A1 (Fig. 1f). However, upon discontinuation of rifabutin, 7 days were necessary for 58% of the individuals to have the CYP3A4 abundance reaching the 1.25-fold threshold (Fig. 1c). UGT1A1 induction by rifabutin was not strong enough to go above this threshold (Fig. 1f).

The residual inducing effect of efavirenz was predicted to decrease the raltegravir AUC_{τ} by 16%, 7%, and 3% at days 1, 7, and 14 post-dosing. The C_{trough} was reduced by 24%, 11%, and 5% on days 1, 7, and 14 post-dosing (Table 2). Seven days were necessary to return to UGT1A1 baseline enzyme levels.

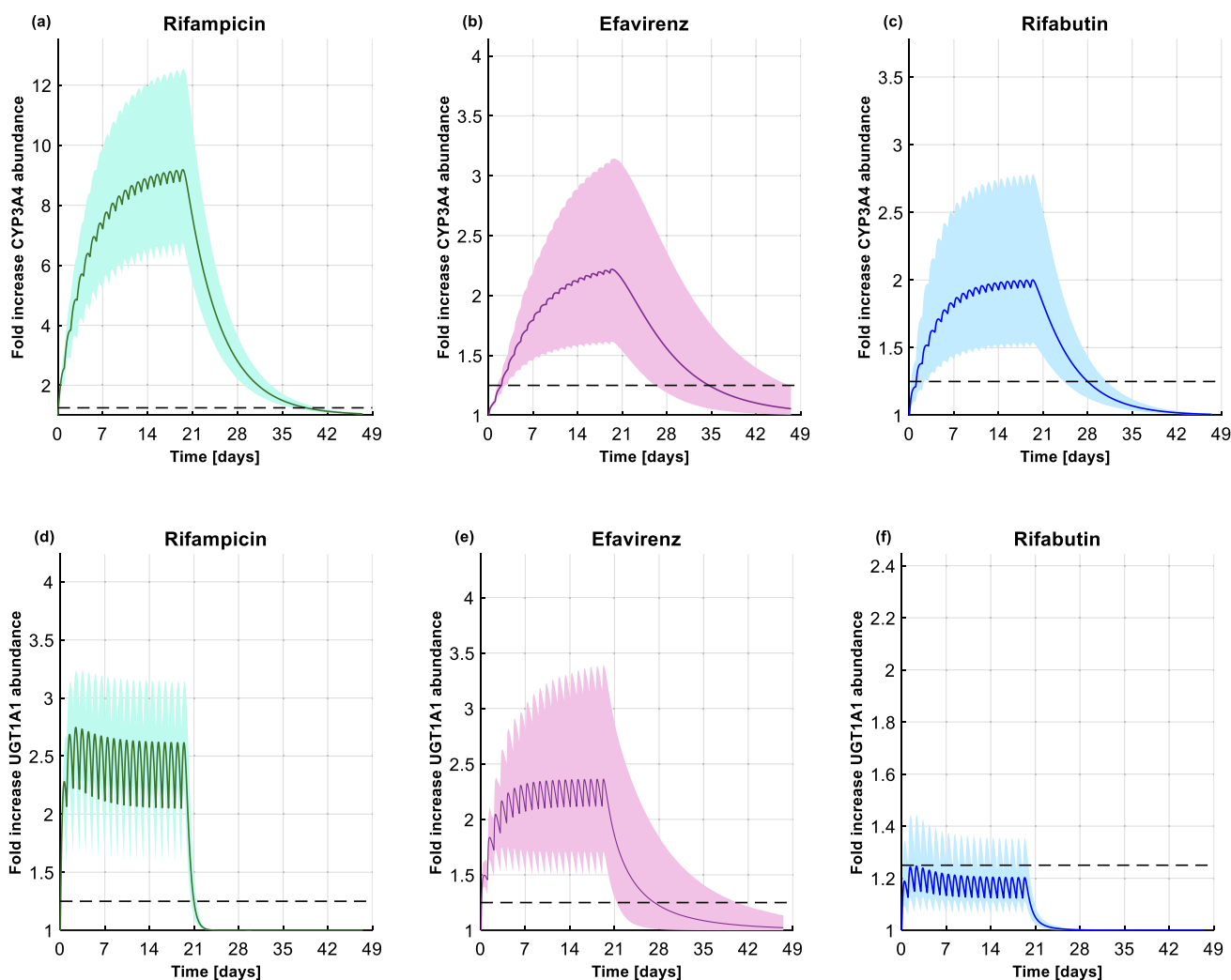


Fig. 1 Fold increase in hepatic CYP3A4 abundance upon initiation and discontinuation of **a** rifampicin (600 mg once daily), **b** efavirenz (600 mg once daily), and **c** rifabutin (300 mg once daily). Fold increase in hepatic UGT1A1 abundance upon initiation and discontinuation of **d** rifampicin (600 mg once daily), **e** efavirenz (600 mg once daily), and **f** rifabutin (300 mg once daily). In all the fig-

ures, the *solid line*, the shaded area, and the *dashed line* represent the mean, the 90% normal range, and the 1.25-fold cut-off threshold above which the AUC ratio (i.e., in the presence vs. the absence of an inducer) is below 0.8. *CYP* cytochrome P450; *UGT* uridine diphosphate glucuronosyltransferase; *AUC* area under the concentration-time curve

3.4 Sensitivity Analysis

Modifying the K_{deg} of UGT1A1 by 1% resulted in sensitivity coefficients for AUC and C_{trough} at days 1, 7, 14, and 28 post-rifampicin dosing which were lower than 0.1, thereby reflecting a low model uncertainty.

4 Discussion

Contemporary first-line ARVs have a lower potential to cause DDIs; however, these agents can be impacted by other co-medications that a PLWH may be taking, notably those with inducing properties. Thus, the characterization of the

onset and disappearance of induction is warranted, not only for the appropriate management of DDIs in clinical practice but also for the correct design of clinical studies.

To date, the onset and disappearance of CYP3A4 enzyme induction has only been characterized for rifampicin. Using PBPK modeling, Kapetas et al. notably showed that the maximal induction of CYP3A4 was achieved faster in the intestine compared to the liver, for which at least a 10-day rifampicin treatment course was needed before reaching maximal induction [11]. Our simulations with rifampicin are in line with the study by Kapetas et al., since hepatic CYP3A4 was predicted to require approximately 14 days to reach near-maximal induction and 18 days to return to baseline abundance after stopping rifampicin. We did not

Table 2 Predicted effect of residual induction on raltegravir pharmacokinetics at days 1, 7, 14, and 28 post-rifampicin, efavirenz, and rifabutin dosing

	Absence inducer	After stopping inducer	DDI ratio (residual induction)
Raltegravir—day 1 after stopping rifampicin			
C_{trough} [ng/mL]	107 (69)	84 (51)	0.78
$AUC_{0-\tau}$ [ng×h/mL]	7312 (38)	6192 (30)	0.85
Raltegravir—day 7 after stopping rifampicin			
C_{trough} [ng/mL]	128 (76)	128 (76)	1.00
$AUC_{0-\tau}$ [ng×h/mL]	7740 (41)	7739 (41)	1.00
Raltegravir—day 14 after stopping rifampicin			
C_{trough} [ng/mL]	128 (76)	128 (76)	1.00
$AUC_{0-\tau}$ [ng×h/mL]	7740 (41)	7740 (41)	1.00
Raltegravir—day 28 after stopping rifampicin			
C_{trough} [ng/mL]	128 (76)	128 (76)	1.00
$AUC_{0-\tau}$ [ng×h/mL]	7740 (41)	7740 (41)	1.00
Raltegravir—day 1 after stopping efavirenz			
C_{trough} [ng/mL]	108 (83)	82 (49)	0.76
$AUC_{0-\tau}$ [ng×h/mL]	7357 (40)	6191 (28)	0.84
Raltegravir—day 7 after stopping efavirenz			
C_{trough} [ng/mL]	129 (82)	115 (71)	0.89
$AUC_{0-\tau}$ [ng×h/mL]	7777 (42)	7243 (38)	0.93
Raltegravir—day 14 after stopping efavirenz			
C_{trough} [ng/mL]	129 (82)	123 (79)	0.95
$AUC_{0-\tau}$ [ng×h/mL]	7778 (42)	7547 (41)	0.97
Raltegravir—day 28 after stopping efavirenz			
C_{trough} [ng/mL]	129 (82)	127 (83)	0.99
$AUC_{0-\tau}$ [ng×h/mL]	7778 (42)	7716 (42)	0.99
Raltegravir—day 1 after stopping rifabutin			
C_{trough} [ng/mL]	107 (82)	102 (79)	0.95
$AUC_{0-\tau}$ [ng×h/mL]	7336 (40)	7098 (38)	0.97
Raltegravir—day 7 after stopping rifabutin			
C_{trough} [ng/mL]	128 (82)	128 (82)	1.00
$AUC_{0-\tau}$ [ng×h/mL]	7553 (42)	7744 (42)	1.00
Raltegravir—day 14 after stopping rifabutin			
C_{trough} [ng/mL]	128 (82)	128 (82)	1.00
$AUC_{0-\tau}$ [ng×h/mL]	7554 (42)	7753 (42)	1.00
Raltegravir—day 28 after stopping rifabutin			
C_{trough} [ng/mL]	128 (82)	128 (82)	1.00
$AUC_{0-\tau}$ [ng×h/mL]	7554 (42)	7754 (42)	1.00

The results are represented as geometric mean (CV)

$AUC_{0-\tau}$ area under the concentration–time curve to tau; C_{trough} trough concentration; *DDI* drug–drug interaction

evaluate the induction of intestinal CYP3A4 given that the time to reach maximal induction and de-induction was shown to be quick in the study by Kapetas et al. [11]. The more rapid disappearance of induction in the intestine compared to the liver is explained by the K_{deg} of the enzyme which is equal to 0.03 h^{-1} for intestinal CYP3A4 [9] and

0.0077 h^{-1} for hepatic CYP3A4 [9]. Our simulations are also supported by clinical data and PBPK modeling studies reporting that induction can take up to 14 days to reach maximal effect [11, 12, 35–43]. In addition, our predictions are consistent with studies evaluating the change in biomarkers (i.e., 6-beta-hydroxy-cortisol excretion and the 6-beta-hydroxy-cortisol/cortisol ratio) at baseline (pre-inducer administration), during the administration of rifampicin, and after stopping the inducer [44, 45]. Our predictions showed that 18 days are necessary to return to baseline CYP3A4 enzyme levels. Our results are consistent with the results published by Reitman et al. [46]. The authors showed that 28 days were enough to completely washout the residual inducing effect of rifampicin on midazolam, since 15 days post-discontinuation of rifampicin, midazolam AUC, and C_{max} , were still reduced by 19% and 27%, respectively. However, the authors concluded that the residual inducing effect observed after 15 days may not be clinically significant [46]. Baneyx et al. also demonstrated that the time to return to baseline enzyme levels for CYP3A4 is 15 days [42].

Dolutegravir and raltegravir were chosen as victim drugs in our study to investigate the effect on UGT1A1. Of interest, maximal UGT1A1 induction was achieved faster upon initiation of rifampicin compared to CYP3A4 (Fig. 1a and d). In contrast to CYP3A4, no studies have evaluated the change in UGT1A1 abundance during and after stopping rifampicin. However, a clinical study evaluated the level of bilirubin glucuronidation (UGT1A1 substrate [47]). The clinical study showed that the level of bilirubin conjugation increased at the beginning of the treatment, with rifampicin reaching a plateau after 6 days. On the other hand, upon discontinuation of rifampicin, the level of bilirubin glucuronidation ratios were still significantly higher, indicating that the UGT1A1 activity did not return to baseline level, which could possibly also be explained by lifestyle factors [43]. Another clinical study investigating the DDI between dolutegravir and rifampentine (strong CYP3A4 and UGT1A1 inducer [48]) showed decreases in dolutegravir C_{trough} of 23%, 64%, and 56% at days 1, 2 and 6 post-rifampentine administration [48]. Given that UGT1A1 is the major enzyme involved in dolutegravir and raltegravir metabolism, these observed clinical data are supportive of the fast UGT1A1 induction upon initiation of a strong inducer, similar to our model prediction. On the other hand, after discontinuation of rifampicin, our simulations show that the residual inducing effect led to a decrease of 60% in dolutegravir C_{trough} . A similar dolutegravir C_{trough} reduction has been reported in a clinical study after discontinuation of rifampentine (another strong inducer), in which dolutegravir C_{trough} was still reduced by 56% at day 6 post-rifampentine administration [48]. Although our simulations indicate a rapid return to UGT1A1 baseline enzyme level, the longer period for dolutegravir C_{trough} recovery could relate to CYP3A4, which contributes to dolutegravir

metabolism and which requires more time to recover from induction. Thus, our findings for UGT1A1 pure substrates should be interpreted with caution, since the K_{deg} value for UGT1A1 was derived from an animal model and therefore may not be extrapolated to humans.

There is a paucity of data on the timeline of induction for moderate inducers such as efavirenz and rifabutin. Based on our results, rifabutin needs at least 7 days to attain near-maximal CYP3A4 induction, while efavirenz needs at least 14 days. After stopping their administration, rifabutin needs 7 days to return to baseline, while efavirenz needs 14 days. These distinct timelines relate to their different plasma concentrations at the time of stopping their administration. Twenty-four hours after stopping rifabutin, its plasma concentration is lower than its half-maximal inhibitory concentration (IC_{50}) (i.e., $0.3 \mu\text{M}$ [49]), and therefore the induction effect is minimal. In contrast, 24 h after stopping efavirenz, its concentration is still above its IC_{50} (i.e., $3.9 \mu\text{M}$ [50]), and the concentration remains for at least another week around the IC_{50} value, causing a persisting inducing effect on co-administered drugs. As for rifampicin, the onset of UGT1A1 induction was faster than CYP3A4 upon initiating efavirenz or rifabutin. The DDI between efavirenz and raltegravir has been studied in a clinical trial and, to ensure full induction of UGT1A1, the authors decided to administer efavirenz for 12 days [25]. However, based on Fig. 1e, 7 days would have been sufficient to have near-full induction of UGT1A1. As for CYP3A4, the residual inducing effect on UGT1A1 lasts longer for efavirenz compared to rifabutin, given that the plasma concentration of efavirenz is close to its IC_{50} .

Altogether, available data and the results of our study support the common practice to maintain the adjusted dosage of ARVs for another 2 weeks after the last dose of the inducer. Although our simulations suggest that this time window could be shortened to 1 week after stopping rifabutin, it is preferable to recommend 2 weeks for all inducers, not only to prevent errors but also because the concentrations of inducers, which impact the offset of induction, are not routinely measured. Furthermore, it should be emphasized that the resolution of induction may last longer in some individuals, as demonstrated in clinical trials with CYP3A4 substrates [46, 51], and as indicated by the large variability in enzyme fold-induction of CYP3A4 and UGT1A1 in our virtual cohort representing the healthy Caucasian population (Fig. 1). Our predictions are also supported by the large variability observed in clinical trials [52].

Several limitations should be acknowledged. First, given the limited clinical data for the effect of different inducers on the change in CYP3A4 and UGT1A1 enzyme abundance, we could not fully evaluate our whole-body PBPK model. However, the PBPK model was extensively verified prior to simulating unstudied scenarios, and therefore we are confident that our conclusions are correct. Second, the paucity of

biological data for UGT enzymes, particularly data regarding the degradation rate constant in humans, are missing, which is the reason why our in-house PBPK model uses a K_{deg} value for UGT1A1 enzyme derived from animal model [32]. Despite this limitation, the sensitivity analysis for this parameter shows a low model uncertainty, but, nevertheless, future studies should determine this parameter in humans.

5 Conclusions

This study indicates that at least 14 days are necessary to reach the CYP3A4 maximal inducing effect, and to return to baseline enzyme levels upon initiation and discontinuation of an inducer. The induction and de-induction processes are predicted to be faster for UGT1A1. The main driving parameters for onset and resolution of induction include the degradation rate constant of the enzyme, the inducer strength, and its half-life and related concentrations after stopping the administration. Available data and the findings of this study support the common practice to maintain the adjusted dosage of the ARVs for another 2 weeks after stopping an inducer. The findings of this work are particularly relevant for low- and middle-income countries given the HIV/TB syndemic often requiring rifampicin to be initiated and subsequently discontinued in individuals on first-line dolutegravir-containing regimens.

Supplementary Information The online version contains supplementary material available at <https://doi.org/10.1007/s13318-023-00833-9>.

Declarations

Funding Open access funding provided by University of Basel. This study was supported by the Swiss National Foundation (Grant number: 188504).

Conflicts of interest CM has received speaker honoraria from MSD, ViiV and Pfizer unrelated to this work. All other authors have no conflicts of interest relevant to the content of this study.

Ethics approval Not applicable.

Availability of data and material The data that support the findings of this study are available upon reasonable request to the corresponding author.

Code availability May be available upon reasonable request to the corresponding author.

Consent to participate Not applicable.

Consent for publication Not applicable.

Authors contributions SB collected the data, ran the simulations, analysed the data, and wrote the first draft of the manuscript. MBe contributed to the data analysis and writing of the manuscript. FS provided modelling input and supervised the data analysis. MBa provided

clinical input. CM designed the study, supervised the data analysis, provided clinical input and obtained the funding. All authors contributed to the critical review and approval of the manuscript.

Open Access This article is licensed under a Creative Commons Attribution-NonCommercial 4.0 International License, which permits any non-commercial use, sharing, adaptation, distribution and reproduction in any medium or format, as long as you give appropriate credit to the original author(s) and the source, provide a link to the Creative Commons licence, and indicate if changes were made. The images or other third party material in this article are included in the article's Creative Commons licence, unless indicated otherwise in a credit line to the material. If material is not included in the article's Creative Commons licence and your intended use is not permitted by statutory regulation or exceeds the permitted use, you will need to obtain permission directly from the copyright holder. To view a copy of this licence, visit <http://creativecommons.org/licenses/by-nc/4.0/>.

References

- Trickey A, Sabin CA, Burkholder G, Crane H, d'Arminio Monforte A, Egger M, et al. Life expectancy after 2015 of adults with HIV on long-term antiretroviral therapy in Europe and North America: a collaborative analysis of cohort studies. *Lancet HIV*. 2023;10(5):e295–307.
- Back D, Marzolini C. The challenge of HIV treatment in an era of polypharmacy. *J Int AIDS Soc*. 2020;23(2): e25449.
- Urquhart BL, Tirona RG, Kim RB. Nuclear receptors and the regulation of drug-metabolizing enzymes and drug transporters: implications for interindividual variability in response to drugs. *J Clin Pharmacol*. 2007;47(5):566–78.
- Mangelsdorf DJ, Thummel C, Beato M, Herrlich P, Schutz G, Umesono K, et al. The nuclear receptor superfamily: the second decade. *Cell*. 1995;83(6):835–9.
- Crauwels H, Vingerhoets J, Ryan R, Witek J, Anderson D. Pharmacokinetic parameters of once-daily rilpivirine following administration of efavirenz in healthy subjects. *Antivir Ther*. 2012;17(3):439–46.
- U.S. Food and Drug Administration. Tivicay product label. 2013; Available from: https://www.accessdata.fda.gov/drugsatfda_docs/label/2013/204790lbl.pdf. Accessed 21 Dec 2022
- U.S. Food and Drug Administration. Isentress product label. 2007; Available from: https://www.accessdata.fda.gov/drugsatfda_docs/label/2011/022145s018lbl.pdf. Accessed 21 Dec 2022
- U.S. Food and Drug Administration. Pifeltro product label. 2018; Available from: https://www.accessdata.fda.gov/drugsatfda_docs/label/2018/210806s000lbl.pdf. Accessed 21 Dec 2022
- Rowland Yeo K, Walsky RL, Jamei M, Rostami-Hodjegan A, Tucker GT. Prediction of time-dependent CYP3A4 drug-drug interactions by physiologically based pharmacokinetic modelling: impact of inactivation parameters and enzyme turnover. *Eur J Pharm Sci*. 2011;43(3):160–73.
- Almond LM, Mukadam S, Gardner I, Okialda K, Wong S, Hatley O, et al. Prediction of drug-drug interactions arising from CYP3A induction using a physiologically based dynamic model. *Drug Metab Dispos*. 2016;44(6):821–32.
- Kapetas AJ, Sorich MJ, Rodrigues AD, Rowland A. Guidance for rifampin and midazolam dosing protocols to study intestinal and hepatic cytochrome P450 (CYP) 3A4 induction and de-induction. *AAPS J*. 2019;21(5):78.
- Kinzig H, Stader F, Bunglawala FS, Rajoli R, Cottura N, Howarth AE, et al. High-dose rifampicin for the treatment of leprosy in HIV patients taking dolutegravir [abstract n. 450]. Conference on Retroviruses and Opportunistic Infections. Boston, Massachusetts, USA; March 8–11, 2020.
- Song I, Borland J, Chen S, Lou Y, Peppercorn A, Wajima T, et al. Effect of atazanavir and atazanavir/ritonavir on the pharmacokinetics of the next-generation HIV integrase inhibitor, S/GSK1349572. *Br J Clin Pharmacol*. 2011;72(1):103–8.
- Moss DM, Siccardi M, Back DJ, Owen A. Predicting intestinal absorption of raltegravir using a population-based ADME simulation. *J Antimicrob Chemother*. 2013;68(7):1627–34.
- U.S. Food and Drug Administration. Rifadin product label. 2010; Available from: https://www.accessdata.fda.gov/drugsatfda_docs/label/2010/050420s073,050627s012lbl.pdf. Accessed 21 Dec 2022
- U.S. Food and Drug Administration. Sustiva product label. 1998; Available from: https://www.accessdata.fda.gov/drugsatfda_docs/label/2011/020972s038lbl.pdf. Accessed 21 Dec 2022
- Pfizer Canada ULC. Product Monograph Mycobutin (rifabutin capsule USP). 2003; Available from: https://www.pfizer.ca/sites/default/files/202102/MYCOBUTIN_PM_E_244143_11Feb2021.pdf. Accessed 21 Dec 2022
- Stader F, Penny MA, Siccardi M, Marzolini C. A comprehensive framework for physiologically based pharmacokinetic modelling in Matlab(R). *CPT Pharmacometrics Syst Pharmacol*. 2019;8(7):444–59.
- Stader F, Siccardi M, Battegay M, Kinzig H, Penny MA, Marzolini C. Repository describing an aging population to inform physiologically based pharmacokinetic models considering anatomical, physiological, and biological age-dependent changes. *Clin Pharmacokinet*. 2019;58(4):483–501.
- Stader F, Courlet P, Kinzig H, Battegay M, Decosterd LA, Penny MA, et al. Effect of ageing on antiretroviral drug pharmacokinetics using clinical data combined with modelling and simulation. *Br J Clin Pharmacol*. 2021;87(2):458–70.
- Bettonte Berton M, Stader F, Battegay M, Marzolini C. Management of drug-drug interactions between long-acting cabotegravir and rilpivirine and comedication with inducing properties: a modelling study. *Clin Infect Dis*. 2022;76:1225.
- Dooley KE, Sayre P, Borland J, Purdy E, Chen S, Song I, et al. Safety, tolerability, and pharmacokinetics of the HIV integrase inhibitor dolutegravir given twice daily with rifampin or once daily with rifabutin: results of a phase 1 study among healthy subjects. *J Acquir Immune Defic Syndr*. 2013;62(1):21–7.
- Song I, Borland J, Chen S, Guta P, Lou Y, Wilfret D, et al. Effects of enzyme inducers efavirenz and tipranavir/ritonavir on the pharmacokinetics of the HIV integrase inhibitor dolutegravir. *Eur J Clin Pharmacol*. 2014;70(10):1173–9.
- Taburet AM, Sauvageon H, Grinsztejn B, Assuied A, Veloso V, Pilotto JH, et al. Pharmacokinetics of raltegravir in HIV-infected patients on rifampicin-based antitubercular therapy. *Clin Infect Dis*. 2015;61(8):1328–35.
- Krishna R, East L, Larson P, Siringhaus T, Herpok L, Bethel-Brown C, et al. Efavirenz does not meaningfully affect the single dose pharmacokinetics of 1200 mg raltegravir. *Biopharm Drug Dispos*. 2016;37(9):542–9.
- Brainard DM, Kassahun K, Wenning LA, Petry AS, Liu C, Lunceford J, et al. Lack of a clinically meaningful pharmacokinetic effect of rifabutin on raltegravir: in vitro/in vivo correlation. *J Clin Pharmacol*. 2011;51(6):943–50.
- de Wet J, DeJesus E, Sloan L, Koteff J, Brennan C, Adkison K, et al. Pharmacokinetics of dolutegravir after switching to abacavir/dolutegravir/ lamivudine from an efavirenz-based regimen: a PK sub-study from STRIIVING. 17th International Workshop on Clinical Pharmacology of HIV and Hepatitis Therapy. Washington DC; 2016.

28. Shebley M, Sandhu P, Emami Riedmaier A, Jamei M, Narayanan R, Patel A, et al. Physiologically based pharmacokinetic model qualification and reporting procedures for regulatory submissions: a consortium perspective. *Clin Pharmacol Ther.* 2018;104(1):88–110.
29. Abduljalil K, Cain T, Humphries H, Rostami-Hodjegan A. Deciding on success criteria for predictability of pharmacokinetic parameters from in vitro studies: an analysis based on in vivo observations. *Drug Metab Dispos.* 2014;42(9):1478–84.
30. Guest EJ, Aarons L, Houston JB, Rostami-Hodjegan A, Galetin A. Critique of the two-fold measure of prediction success for ratios: application for the assessment of drug-drug interactions. *Drug Metab Dispos.* 2011;39(2):170–3.
31. Hanke N, Frechen S, Moj D, Britz H, Eissing T, Wendl T, et al. PBPK models for CYP3A4 and P-gp DDI prediction: a modeling network of rifampicin, itraconazole, clarithromycin, midazolam, alfentanil, and digoxin. *CPT Pharmacometrics Syst Pharmacol.* 2018;7(10):647–59.
32. Suzuki M, Hirata M, Takagi M, Watanabe T, Iguchi T, Koiwai K, et al. Truncated UDP-glucuronosyltransferase (UGT) from a Crigler-Najjar syndrome type II patient colocalizes with intact UGT in the endoplasmic reticulum. *J Hum Genet.* 2014;59(3):158–62.
33. Lin Z, Monteiro-Riviere NA, Riviere JE. A physiologically based pharmacokinetic model for polyethylene glycol-coated gold nanoparticles of different sizes in adult mice. *Nanotoxicology.* 2016;10(2):162–72.
34. Teegarden JG, Deisinger PJ, Poet TS, English JC, Faber WD, Barton HA, et al. Derivation of a human equivalent concentration for n-butanol using a physiologically based pharmacokinetic model for n-butyl acetate and metabolites n-butanol and n-butyric acid. *Toxicol Sci.* 2005;85(1):429–46.
35. Lee KH, Shin JG, Chong WS, Kim S, Lee JS, Jang IJ, et al. Time course of the changes in prednisolone pharmacokinetics after co-administration or discontinuation of rifampin. *Eur J Clin Pharmacol.* 1993;45(3):287–9.
36. Niemi M, Backman JT, Fromm MF, Neuvonen PJ, Kivistö KT. Pharmacokinetic interactions with rifampicin : clinical relevance. *Clin Pharmacokinet.* 2003;42(9):819–50.
37. Chen J, Stringer R, Shah B, Gu J, Zhang Y, Hackling M, et al. Drug-Drug Interaction Studies to Evaluate the Effect of Inhibition of UGT1A1 and CYP3A4 and Induction of CYP3A4 on the Pharmacokinetics of Tropifexor in Healthy Subjects. *Clin Pharmacol Drug Dev.* 2022;11(11):1253–63.
38. Pithavala YK, Tortorici M, Toh M, Garrett M, Hee B, Kuruganti U, et al. Effect of rifampin on the pharmacokinetics of Axitinib (AG-013736) in Japanese and Caucasian healthy volunteers. *Cancer Chemother Pharmacol.* 2010;65(3):563–70.
39. Fromm MF, Busse D, Kroemer HK, Eichelbaum M. Differential induction of prehepatic and hepatic metabolism of verapamil by rifampin. *Hepatology.* 1996;24(4):796–801.
40. Backman JT, Kivistö KT, Olkkola KT, Neuvonen PJ. The area under the plasma concentration-time curve for oral midazolam is 400-fold larger during treatment with itraconazole than with rifampicin. *Eur J Clin Pharmacol.* 1998;54(1):53–8.
41. Xu Y, Zhou Y, Hayashi M, Shou M, Skiles GL. Simulation of clinical drug-drug interactions from hepatocyte CYP3A4 induction data and its potential utility in trial designs. *Drug Metab Dispos.* 2011;39(7):1139–48.
42. Baneyx G, Parrott N, Meille C, Iliadis A, Lave T. Physiologically based pharmacokinetic modeling of CYP3A4 induction by rifampicin in human: influence of time between substrate and inducer administration. *Eur J Pharm Sci.* 2014;2(56):1–15.
43. Chattopadhyay N, Kanacher T, Casjens M, Frechen S, Ligges S, Zimmermann T, et al. CYP3A4-mediated effects of rifampicin on the pharmacokinetics of vilaprisan and its UGT1A1-mediated effects on bilirubin glucuronidation in humans. *Br J Clin Pharmacol.* 2018;84(12):2857–66.
44. Ohnhaus EE, Breckenridge AM, Park BK. Urinary excretion of 6 beta-hydroxycortisol and the time course measurement of enzyme induction in man. *Eur J Clin Pharmacol.* 1989;36(1):39–46.
45. Tran JQ, Kovacs SJ, McIntosh TS, Davis HM, Martin DE. Morning spot and 24-hour urinary 6 beta-hydroxycortisol to cortisol ratios: intraindividual variability and correlation under basal conditions and conditions of CYP 3A4 induction. *J Clin Pharmacol.* 1999;39(5):487–94.
46. Reitman ML, Chu X, Cai X, Yabut J, Venkatasubramanian R, Zajic S, et al. Rifampin's acute inhibitory and chronic inductive drug interactions: experimental and model-based approaches to drug-drug interaction trial design. *Clin Pharmacol Ther.* 2011;89(2):234–42.
47. Miners JO, Mackenzie PI, Knights KM. The prediction of drug-glucuronidation parameters in humans: UDP-glucuronosyltransferase enzyme-selective substrate and inhibitor probes for reaction phenotyping and in vitro-in vivo extrapolation of drug clearance and drug-drug interaction potential. *Drug Metab Rev.* 2010;42(1):196–208.
48. Dooley KE, Savic R, Gupte A, Marzinke MA, Zhang N, Edward VA, et al. Once-weekly rifapentine and isoniazid for tuberculosis prevention in patients with HIV taking dolutegravir-based antiretroviral therapy: a phase 1/2 trial. *Lancet HIV.* 2020;7(6):e401–9.
49. McGinnity DF, Zhang G, Kenny JR, Hamilton GA, Otmani S, Stams KR, et al. Evaluation of multiple in vitro systems for assessment of CYP3A4 induction in drug discovery: human hepatocytes, pregnane X receptor reporter gene, and Fa2N-4 and Hep-aRG cells. *Drug Metab Dispos.* 2009;37(6):1259–68.
50. Molto J, Rajoli R, Back D, Valle M, Miranda C, Owen A, et al. Use of a physiologically based pharmacokinetic model to simulate drug-drug interactions between antineoplastic and antiretroviral drugs. *J Antimicrob Chemother.* 2017;72(3):805–11.
51. Branch RA, Herman RJ. Enzyme induction and beta-adrenergic receptor blocking drugs. *Br J Clin Pharmacol.* 1984;17(1):77S-84S.
52. Ramsden D, Fung C, Hariparsad N, Kenny JR, Mohutsky M, Parrott NJ, et al. Perspectives from the innovation and quality consortium induction working group on factors impacting clinical drug-drug interactions resulting from induction: focus on cytochrome 3A substrates. *Drug Metab Dispos.* 2019;47(10):1206–21.